# Guanidine Hydrochloride Induced Equilibrium Unfolding Studies of Colicin B and Its Channel-Forming Fragment

H. A. Sathish,[‡] Monica Cusan,[‡] Christopher Aisenbrey,[‡,§] and Burkhard Bechinger*[,‡,§]

*Max-Planck-Institut für Biochemie, Am Klopferspitz 18A, 82152 Martinsried, Germany, and Faculté de chimie, Institut le Bel, 4, rue Blaise Pascal, 67000 Strasbourg, France*

*Received July 30, 2001*

ABSTRACT: The conformational stabilities of full-length colicin B and its isolated C-terminal domain were studied by guanidine hydrochloride induced unfolding. The unfolding/refolding was monitored by far-UV CD and intrinsic tryptophan fluorescence spectroscopies. At pH 7.4, the disruption of the secondary structure of full-length colicin B is monophasic, while changes in tertiary structure occur in two separate transitions. The intermediate species, which is well-populated around 2.2 M guanidine hydrochloride, exhibits secondary and tertiary structures distinct from both native and unfolded states. Whereas the domain structure of native full-length colicin B is reflected in its DSC profile, the folding intermediate of the same protein exhibits a single unresolved peak. These observations have led us to propose an unfolding model for full-length colicin B where the first transition between 0 and 2.5 M GuHCl with an associated free energy of 3 kcal/mol correlates with the partial unfolding of the R/T domain. The stability of full-length colicin B is weakened due to the presence of the R/T domain in both the native [Ortega, A., Lambotte, S., and Bechinger, B. (2001) *J. Biol. Chem. 276* (17), 13563−13572] and the intermediate states. The second transition between 2.5 and 5 M GuHCl involves unfolding of the C-terminal domain ($\Delta G^0_{I\rightarrow U} = 7$ kcal/mol). The isolated colicin B C-terminal domain consists of two subdomains, and the two parts of this protein fragment unfold sequentially through the formation of at least one intermediate. The significance of these results for membrane insertion of colicin B is discussed.

It has been well-recognized that the proper folding of proteins is an important prerequisite for functional integrity. Therefore, several proteins have been studied after denaturation, and models of the folding mechanisms are emerging (*1*−*4*). Protein folding is a directed process, and for proteins >100 residues proceeds through a definite sequence of intermediate states with decreasing Gibbs free energy (*1, 4*). The inverse process is of equal importance, for example, during the insertion and translocation of proteins into and through phospholipid membranes (*5*). Unfortunately, little is known about the structural mechanisms of the controlled unfolding of polypeptides.

It has been proposed that the folding of an extended polypeptide chain starts with its collapse into a more compact globule that will acquire the native state in further steps (*1*). Whereas folding intermediates of a few proteins have been characterized in considerable detail by structural methods (*1, 3, 6, 7*), the transition intermediates are unstable and short-lived and could only be characterized in an indirect manner (*2, 8*). With the limited database available, considerable controversy remains as to the unifying properties of folding or transition intermediates (*1, 4, 9*). For integral membrane proteins, the proposed models reflect the separation of polar and apolar regions of lipid bilayers, albeit with some analogy to those models developed for soluble proteins (*10, 11*). When compared to small globular proteins, very little structural and thermodynamic data are available for membrane proteins.

Stable folding intermediates have been classified as molten globule or pre-molten globule states as well as partially folded domains or subdomains (*1, 3, 12*−*14*). Structural investigations of intermediates show that parts of the molecules adopt nativelike secondary structures, but tertiary contacts between these elements are poorly defined. Given the wide variety of possible folding intermediates, careful characterization is required for understanding the folding/unfolding pathways of multidomain proteins. This, in a first step, requires the identification of conformational states that emerge during folding and unfolding.

Membrane proteins consist of hydrophobic regions in contact with the inner part of lipid bilayers and polar regions interacting with solvent or within the lipid headgroup region (*15*). It is of special interest to study proteins that occur in water-soluble as well as membrane-inserted conformations as these proteins have been shown to undergo profound conformational changes reflecting the different interactions in aqueous and bilayer environments. The characterization of these structural changes, therefore, enables one to better understand not only the interaction contributions important for protein conformation but also the proteins' modes of functioning including channel formation. A first unfolding step already occurs in the water phase, or when in contact

* Correspondence should be addressed to this author at the Faculté de chimie, Institut le Bel, 4, rue Blaise Pascal, 67000 Strasbourg, France. Tel.: +33 3 90 24 14 96, FAX: +33 3 90 24 14 90, E-mail: bechinger@chimie.u-strasbg.fr.

[‡] Max-Planck-Institut für Biochemie.

[§] Institut le Bel.

10.1021/bi0115784 CCC: $22.00 
Published on Web 04/04/2002

with the membrane surface. Therefore, studies of the unfolding intermediates of such amphipathic proteins in aqueous solution are a prerequisite to understand later stages of the membrane protein insertion process.

Several bacterial toxins, including some colicins, diphtheria toxin, or proteins controlling cell survival in higher organisms (*16*), have been shown to adopt water-soluble as well as membrane-inserted conformations (*17*). The bacterial proteins can be prepared in quantitative amounts and are therefore amenable to structural studies. Colicins kill sensitive *E. coli* cells by different types of lethal action including depolarization of cellular membranes and inhibition of DNA and of protein synthesis (*18*). Colicin B is a 55 kDa multidomain protein and belongs to the membrane-interacting family of colicins (*19*). The molecule consists of three domains that correspond to different functions of the protein: outer membrane receptor recognition, translocation (*20*, *21*), and voltage-dependent pore-formation (*22*, *23*). Whereas the C-terminal domain of colicin B is closely related to those channel-forming domains of colicins A and N, colicins B and Ia group together when the usage of the TonB translocation machinery is considered (*20*, *21*). Much work on colicins has been performed to better understand the mechanism of channel formation (*21*, *24*−*27*). It has been shown that before insertion into the membranes the C-terminal domains undergo structural alterations into insertion-competent states [e.g., (*14*)]. This raises a number of questions about the structural organization of these proteins and, more specifically, their channel-forming domains.

The structural stability and/or domain interactions of colicin B (*28*) and of the colicin A pore-forming domain (*29*) have been investigated by thermal unfolding. However, the processes investigated previously are irreversible, and therefore equilibrium thermodynamics cannot be applied. To understand the mechanism of action of membrane proteins, it is of utmost importance to understand the general structure of membrane proteins, their thermodynamic stability, and their domain organization.

In this study, we, therefore, extended previous investigations involving this laboratory (*28*) and followed denaturant-induced protein folding/unfolding of full-length colicin B and its isolated C-terminal domain by using tryptophan fluorescence and CD spectroscopy. The data demonstrate that unfolding of both proteins follows reversible multistate processes involving the formation of at least one intermediate. The intermediate states were identified and further characterized by DSC.[1] The denaturant-induced unfolding intermediate exhibits close similarities to the one which has been suggested to be involved in membrane insertion. Due to the reversibility of the denaturant-induced folding/unfolding equilibria, we were able to perform a quantitative thermodynamic analysis of the process.

## MATERIALS AND METHODS

*Materials.* Ultrapure guanidine hydrochloride and all buffer components were purchased from Sigma (St. Louis, MO). Thermolysin was procured from Calbiochem (La Jolla, CA). All other chemicals were of reagent grade.

*Expression and Protein Purification*. The autotrophic strain *E. coli* JM 101 bearing the plasmid pES3 was used to express colicin B. The C-terminal domain was obtained by digestion of full-length colicin B with thermolysin. The expressed full-length protein and the C-terminal domain were purified following established procedures (*22*, *24*). After gel filtration with a SH Sephacryl R100 column (Amersham Pharmacia Biotech, Freiburg, Germany), the purity of the protein was checked by SDS−polyacrylamide gel electrophoresis.

*Equilibrium Unfolding Experiments.* All the equilibrium unfolding experiments were performed as described by Pace et al. (*30*). Protein stocks were prepared in the following buffers: 20 mM Tris, pH 7.4, or 20 mM acetate, pH 4.0. The final protein solutions in GuHCl were prepared by diluting appropriate volumes of protein and GuHCl stock solutions in the respective buffer. The final protein concentrations were as indicated in the figure legends. All samples were mixed gently and incubated at 25 °C for 3 h. To check the reversibility of unfolding, a solution of protein in the unfolded region was dialyzed in a stepwise manner to remove the denaturant.

*Fluorescence Emission Measurements.* Emission spectra were monitored using a Perkin-Elmer LS-50 luminescence spectrometer equipped with a water-thermostat cell holder. Emission spectra were analyzed over the wavelength range of 300−400 nm with an excitation wavelength of 295 nm. Data reported represent the average of two spectra. Spectra were corrected for background signal contributed by buffer or denaturant. All the spectra were recorded at 25 °C.

*Circular Dichroism Measurements.* CD studies were performed on a Jasco J-715 spectropolarimeter equipped with a thermostated cell holder. CD spectra were recorded in the far-UV region between 200 and 250 nm at 25 °C. All measurements were corrected for buffer and denaturant contributions. Each of the spectra presented was the average of four scans.

*Differential Scanning Calorimetry*. Calorimetric experiments were performed using a Microcal VP-DSC high-sensitivity differential scanning calorimeter. Protein solutions were dialyzed against buffer/GuHCl for at least 12 h. The final dialysate was used as a reference. The protein concentrations were as mentioned in the figure legends. All the protein and buffer solutions were degassed with gentle stirring under vacuum before being loaded into the calorimeter. Experiments were performed over a temperature range of 30−90 °C at a scan rate of 1 °C/min. Normalized heat capacity data were corrected for the buffer baseline. Raw DSC data were processed and analyzed using the Origin software (Microcal, Northampton, MA) provided with the instrument. Results of DSC experiments are described as $C_p$ versus temperature profiles.

*Analysis of Equilibrium Unfolding Data.* The unfolding transition curves were analyzed by procedures published previously (*9*, *30*). In short, the equilibrium unfolding data are described by the following model of unfolding (*31*):

$$N \overset{K_1}{\longleftrightarrow} I \overset{K_2}{\longleftrightarrow} U$$

where N is the protein in its native state, I is the intermediate form, and U is the unfolded state. For each step in the

[1] Abbreviations: DSC, differential scanning calorimetry; GuHCl, guanidine hydrochloride; UV CD, ultraviolet circular dichroism; SDS, sodium dodecyl sulfate; R/T, receptor/translocation; $C_p$, molar heat capacity.

reaction (assigned *i*), the free energy change is assumed to be a linear function of [denaturant]. Thus, changes in the Gibbs free energy at any GuHCl concentration can be obtained using $\Delta G_i = \Delta G^i_{H_2O} + m_i$[denaturant], where $\Delta G^i_{H_2O}$ is defined as the free energy changes in the absence of denaturant and $m_i$ are the denaturant *m* values. The contributions of all states to the total signal amplitude are assumed to be additive: $Y_{obs} = Y_N f_N + Y_I f_I + Y_U f_U$, where $Y_N$, $Y_I$, and $Y_U$ represent the signals associated with each form and $f_X$ are the corresponding fractional values. The Origin software (versions 5.0 or 6.1, Microcal, Northampton, MA), which applied the Marquardt−Levenberg algorithm, was used to fit the unfolding data (*30*).

## RESULTS

The spectral changes associated with the unfolding of full-length colicin B and its C-terminal domain were studied by intrinsic tryptophan fluorescence and circular dichroism at 222 nm. Experiments were performed at two different pH values in order to check the effect of proton activity on structural stability. To attain the unfolding equilibrium at each GuHCl concentration, the protein was incubated in the appropriate buffer for 4 h.

The intrinsic tryptophan fluorescence of the colicins was measured and used to monitor protein unfolding. The protein molecules were excited at 295 nm, and the emission spectra were recorded in the range 300−400 nm. The wavelength of maximum emission, the total intensity (300−400 nm), and the intensity at 320 nm, a wavelength where pronounced changes are observed during unfolding, were analyzed as a function of GuHCl concentration. Figure 1A shows the change in the fluorescence emission maxima of full-length colicin B as a function of GuHCl concentration. The emission maximum is red-shifted from 323 to 343 nm due to the addition of ≥4 M GuHCl, indicating the increased exposure of tryptophan residues to bulk solvent. Notably, the unfolding process is reversible, as renaturation by suitable dilution of fully unfolded protein shows complete recovery of all the spectral features of the native protein (Figure 1A). The results obtained from the fluorescence studies were normalized into apparent fractions using standard equations (*30*). The unfolding curves obtained from fluorescence spectra either by measuring $\lambda_{max}$, the intensity at 320 nm, or the total intensity closely parallel each other. Each data set was fitted to a three-state model as described under Materials and Methods, and the thermodynamic parameters of the equilibrium unfolding of full-length colicin B and its C-terminal domain were obtained (Table 1). Furthermore, the fractions of native, intermediate, and unfolded forms of full-length colicin B were calculated using the resulting thermodynamic parameters (Table 1) and are shown in Figure 1B as a function of GuHCl concentration. At 2.3 M GuHCl, >90% of the protein is in its intermediate form (Figure 1B).

The normalized fluorescence emission maxima at pH 7.4 and 4.0 are plotted as a function of GuHCl concentration in Figure 2A,B, respectively. An excellent fit of experimental data is obtained when using a three-state model. At pH 7.4, the curve obtained by fluorescence spectroscopy is clearly biphasic, indicating the presence of at least one stable intermediate in equilibrium with the native and the unfolded forms of the protein (Figure 2A). The result demonstrates

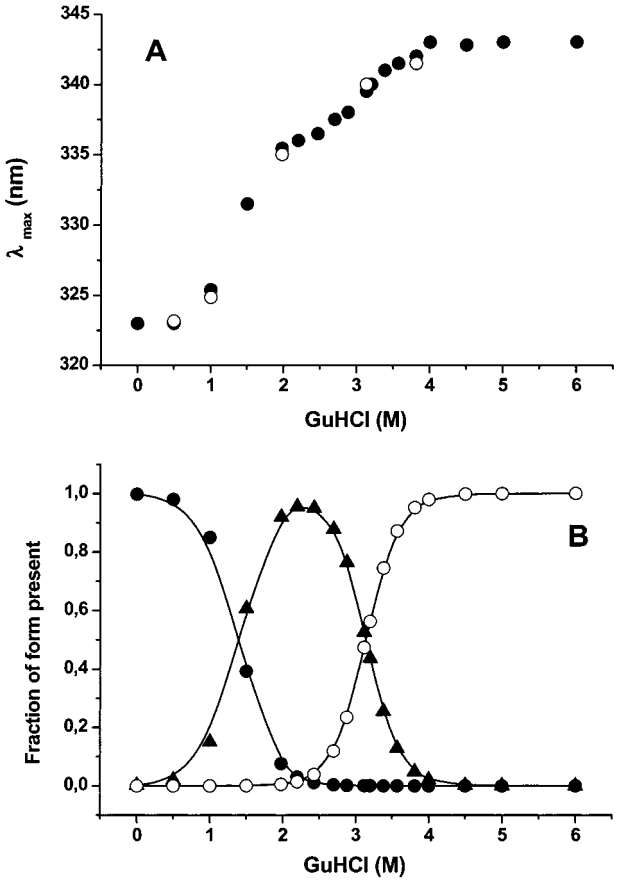


FIGURE 1: (A) GuHCl-induced reversible unfolding of full-length colicin B at pH 7.4 monitored by fluorescence emission maxima. Unfolding (●) and refolding curves (○) are shown. (B) Calculated fractions of native (●), intermediate (▲), and unfolded (○) forms of full-length colicin B as a function of GuHCl concentration. The fractional values of the conformational states were calculated as described under Materials and Methods using the thermodynamic parameters listed in Table 1.

Table 1: Thermodynamic Parameters Obtained from GuHCl-Induced Reversible Unfolding of Full-Length Colicin B and Its Isolated C-Terminal Domain As Monitored by Fluorescence and Far-UV CD Measurements[a]

| colicin B full protein | method | $\Delta G^0_{N\rightarrow I}$ (kcal/mol) | $\Delta G^0_{I\rightarrow U}$ (kcal/mol) | $m_{N\rightarrow I}$ (kcal mol$^{-1}$ M$^{-1}$) | $m_{I\rightarrow U}$ (kcal mol$^{-1}$ M$^{-1}$) |
|---|---|---|---|---|---|
| pH 7.4 | Flu | 3.2 ± 0.3 | 7.0 ± 1.0 | 2.3 ± 0.2 | 2.1 ± 0.4 |
| | CD | 4.6 ± 0.3 | 5.6 ± 0.4 | 2.9 ± 0.2 | 1.9 ± 0.2 |
| pH 4.0 | Flu | 3.9 ± 0.2 | 8.0 ± 0.3 | 2.0 ± 0.2 | 2.4 ± 0.3 |
| | CD | 2.8 ± 0.6 | 3.7 ± 0.5 | 2.0 ± 0.4 | 1.4 ± 0.2 |
| C-domain, pH 7.4 | Flu | 2.3 ± 0.8 | 2.7 ± 0.3 | 1.7 ± 0.7 | 1.0 ± 0.1 |
| | CD | | 3.3 ± 0.2 | | 1.1 ± 0.1 |
| pH 4.0 | Flu | 3.4 ± 0.5 | 2.1 ± 0.2 | 2.5 ± 0.4 | 2.0 ± 0.1 |
| | CD | | NA | | NA |

[a] Unfolding curves were analyzed using a three-state model as described under Materials and Methods to afford measures of the cardinal thermodynamic parameters. Errors are results of the nonlinear least-squares analysis (CD) or represent estimates obtained from comparing line fits of $\lambda_{max}$, intensity at 320 nm, and total intensity values (Flu). NA, not analyzed.

the sequential unfolding of the protein at pH 7.4, with a first transition between 0 and 2 M GuHCl. The free energy change, $\Delta G^0_{N\rightarrow I}$, and the denaturant *m* value associated with the first transition are 3.2 kcal/mol and 2.3 kcal mol$^{-1}$ M$^{-1}$, respectively (Table 1). The second transition is observed

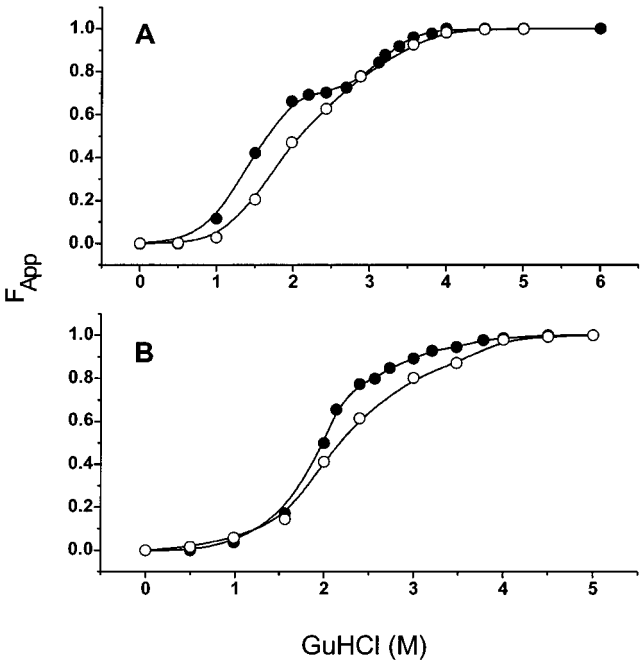


FIGURE 2: GuHCl-induced unfolding of full-length colicin B and noncoincidence of equilibrium unfolding data. The changes in fluorescence emission maxima (●) and the alterations of circular dichroism at 222 nm (○) are shown in a normalized fashion. At pH 7.4 (A) and at pH 4.0 (B). The solid lines are fits obtained by the three-state model as described under Materials and Methods.

between 2.5 and 6 M GuHCl accompanied with a free energy change ($\Delta G^0_{N\rightarrow I}$) of 7 kcal/mol and a denaturant *m* value of 2.1 kcal mol$^{-1}$ M$^{-1}$. Although at pH 4.0 the biphasic behavior is less apparent, the sigmoidal transition is characterized by a small plateau around 2.5 M GuHCl, indicating the presence of a folding intermediate at these GuHCl concentrations (Figure 2B).

To check the effect of [GuHCl] on the secondary structure of colicin B, the unfolding transition was also monitored by far-UV CD. The CD spectrum of the protein was measured in the presence of different concentrations of GuHCl. Figure 2 shows the changes in $\theta_{222}$ values as a function of GuHCl concentration, along with the unfolding curves obtained by fluorescence measurements. In contrast to the fluorescence data, the unfolding curves obtained by CD spectroscopy appear monophasic (Figure 2A,B). Although the intermediate state is not easily recognized in CD measurements, the noncoincidence of fluorescence and CD spectroscopic data is a safe indicator of its presence.

Thus, fluorescence and CD spectroscopic studies indicate that the unfolding of full-length colicin B proceeds through formation of a stable intermediate. Figure 3A,B shows fluorescence and CD spectra of full-length colicin B in its native condition, in its intermediate form, and at 5 M GuHCl. Both the fluorescence intensity and the emission maximum of the intermediate are different from those of the native or the unfolded protein (Figure 3A). Also the circular dichroism of the folding intermediate at 222 nm is decreased by about 40%, indicating partial unfolding and disruption of considerable secondary structure when compared with the native protein (Figure 3B).

To further characterize the intermediate conformation, DSC studies of full-length colicin B were performed. Under the conditions used, the thermal denaturation is irreversible

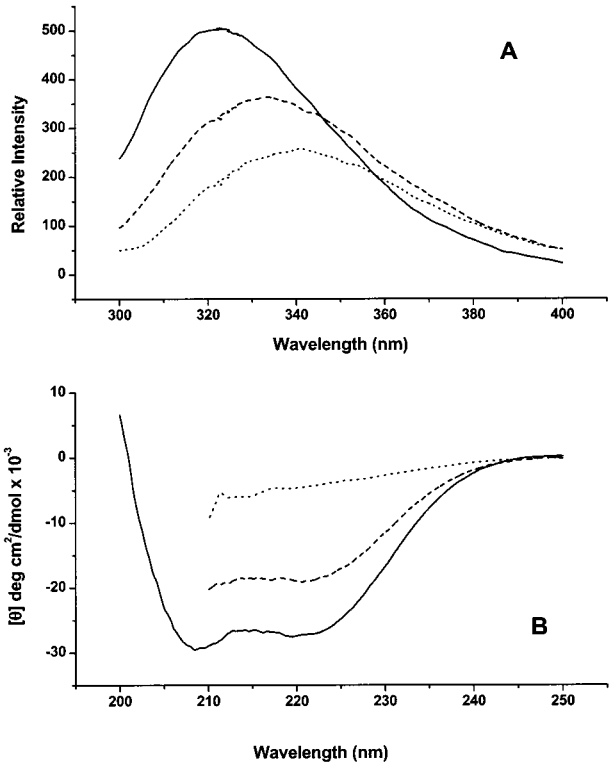


FIGURE 3: Fluorescence and circular dichroism spectra of native full-length colicin B, the folding intermediate, and the unfolded protein. (A) Fluorescence emission spectra were recorded in the range 300−400 nm with an excitation wavelength of 295 nm at a protein concentration of 1.6 $\mu$M in 20 mM Tris-HCl, pH 7.4. (B) CD spectra of 5 $\mu$M full-length colicin B in 20 mM Tris-HCl, pH 7.4. Spectra were recorded at 25 °C in the absence of denaturant (solid line), as well as in the presence of 2 M (dashed line) or 5 M GuHCl (dotted line).

since the calorimetric profile cannot be reproduced during a second heating scan after cooling. Figure 4A shows the DSC profile of full-length colicin B at pH 7.4. In agreement with earlier studies (*28*), the unfolding is characterized by two peaks, a first thermal transition at 54.2 ± 0.5 and a second smaller thermal transition at 60.4 ± 0.5 °C (Table 2). The data can be easily fitted to a multistate model. The DSC unfolding profile of the intermediate form of full-length colicin B is characterized by a single unresolved peak (Figure 4B). However, the peak observed is broad and, when compared to the native state, characterized by a sharp decrease in the thermal transition temperature. Good fits are obtained by either a two-state or a multistate analysis of the thermograms with thermal transition temperatures around 39 °C.

Unfolding of the isolated C-terminal domain was also monitored by fluorescence and far-UV CD measurements. The unfolding curve monitored by changes in the fluorescence spectra shows a broad sigmoidal curve for both pH 7.4 and pH 4.0 (Figure 5A,B, respectively). At pH 7.4, a small plateau is observed around 3.5 M GuHCl. Figure 5A also shows the unfolding of the C-terminal domain as followed by CD spectroscopy. The noncoincidence of the transition curves obtained by fluorescence and CD spectroscopic studies indicates the presence of a folding intermediate. The thermodynamic parameters derived from the three-state model at different pHs for both full-length colicin B and its C-terminal domain are summarized in Table 1.

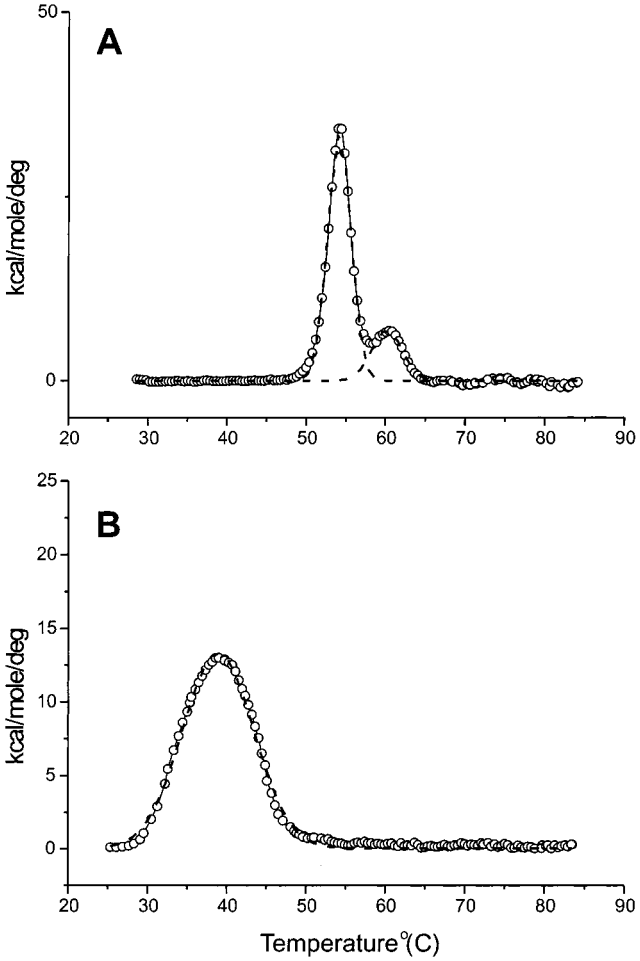


FIGURE 4: Differential scanning calorimetric denaturation endotherm of full-length colicin B. Here (○) represents the experimentally obtained resolution of data. (A) shows the endotherm in the absence of denaturant, and (B) in the presence of 2 M GuHCl. The protein concentration was 25 $\mu$M in 20 mM Tris-HCl, pH 7.4. The individual contributions obtained from Gaussian line-fitting are also shown (dashed lines).

Table 2: Thermodynamic Parameters of Full-Length Colicin B and Its C-Terminal Domain Obtained from DSC Studies

| | $T_m^1$ (°C) | $\Delta H_{cal}^1$ (kcal/mol) | $T_m^2$ (°C) | $\Delta H_{cal}^2$ (kcal/mol) |
|---|---|---|---|---|
| full-length colicin B (native) | 54.2 | 129 | 60.4 | 30 |
| full-length colicin B (I), 2 M GuHCl | | | 38.9 | 146 |
| C-terminal domain (N) | 55.8 | 5 | 66.2 | 33 |
| C-terminal domain (I), 3.2 M GuHCl | | | 58.5 | 15 |

DSC was used to further characterize the colicin B C-terminal domain (*28*) and its GuHCl-induced unfolding intermediate. Again, the thermal unfolding followed by DSC was irreversible. Interestingly, also for this protein two distinct peaks are observed in the absence of denaturant, indicating the presence of more than one unfolding entity (Figure 6A). The first minor peak is characterized by a thermal transition temperature of 55.8 ± 0.5 °C, and a second major transition occurs at 66.2 ± 0.5 °C (Table 2). In contrast, in the presence of 3.5 M GuHCl, the DSC profile of the C-terminal domain of colicin B shows a single peak with a maximum of the excess molar heat capacity at

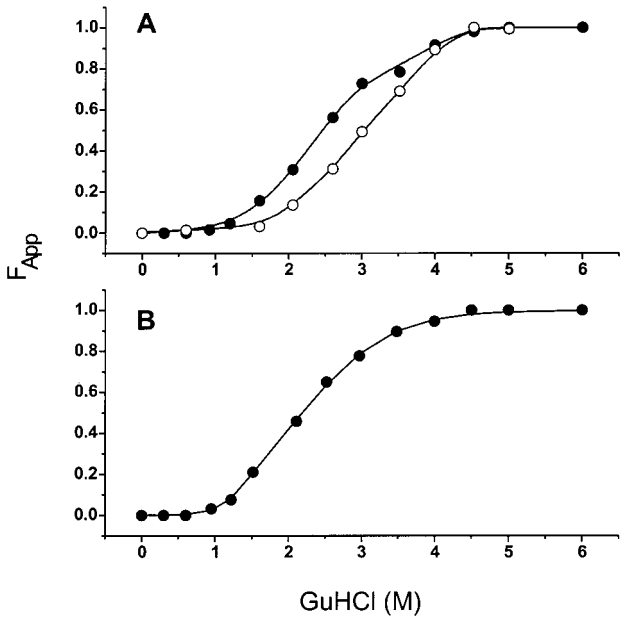


FIGURE 5: GuHCl-induced unfolding of the colicin B C-terminal domain. The changes in fluorescence emission maxima (●) and the alterations of circular dichroism at 222 nm (○) are shown in a normalized fashion. Protein concentrations of 1.5 and 4 $\mu$M were used for fluorescence and CD spectroscopic experiments, respectively. (A) At pH 7.4 and (B) at pH 4.0. The data were fitted to a three-state model as described under Materials and Methods.

58.5 ± 0.5 °C. Although the thermogram could be reasonably well fitted with a simple two-state model, the fit improved by deconvolution into two transitions (Figure 6B).

## DISCUSSION

Many membrane proteins and most peptides experience large conformational changes upon interaction with the membrane surface (*32*). Similarly, posttranslational protein insertion and translocation into and across the membrane require the refolding of proteins when entering or exiting the membrane. To understand these processes, it is important to identify and characterize the respective folding intermediates. Denaturant-induced unfolding allows one to identify those regions that are less stable and therefore best suited to initiate unfolding. Furthermore, due to the reversibility of this process, the equilibrium thermodynamics of the folding/unfolding process can be analyzed. In this paper, we have characterized the conformational stability of full-length colicin B and its isolated C-terminal domain in the presence of GuHCl using fluorescence and far-UV CD spectroscopies as well as differential scanning calorimetry.

*Identification of Folding Intermediates.* Full-length colicin B at pH 7.4 exhibits biphasic unfolding curves when monitored by fluorescence spectroscopy (Figure 1A). This result indicates the presence of at least one stable intermediate during its reversible unfolding reaction (Figure 1B). The three-state model (N ↔ I ↔ U) is confirmed by nonsuperimposable transitions observed with CD and fluorescence spectroscopy (*9*), thereby reflecting the differential sensitivity of CD and fluorescence spectroscopy for secondary and tertiary structural changes, respectively (Figure 2).

In a related manner, previous studies have demonstrated that the DSC profile of full-length colicin B exhibits two well-separated transitions, suggesting thermal denaturation

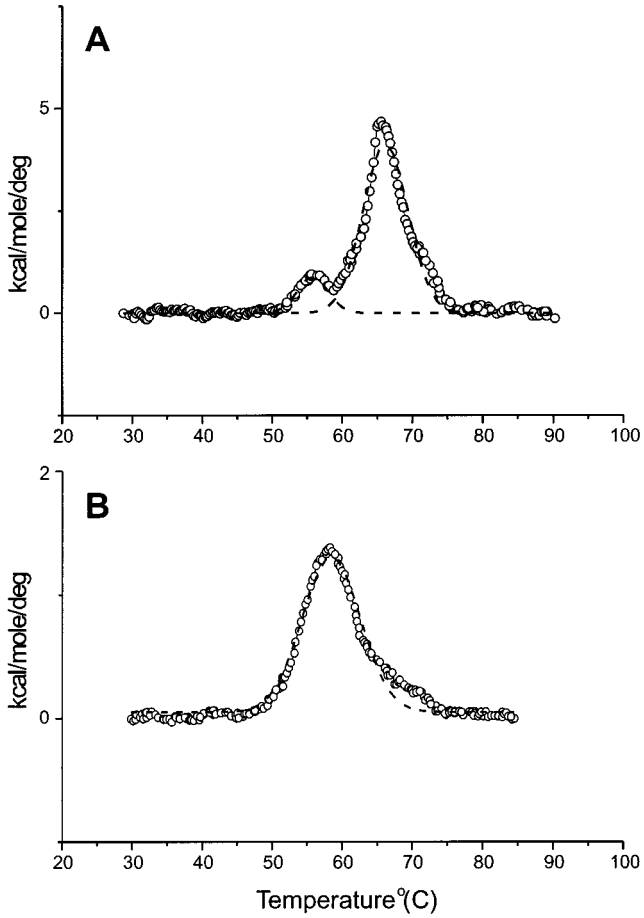


FIGURE 6: Differential scanning calorimetric denaturation endotherm of the colicin B C-terminal domain in the absence (A) and in the presence of 3.5 M GuHCl (B). Here (○) represents the experimentally observed data. The protein concentration was 21 $\mu$M in 20 mM Tris-HCl, pH 7.4. The individual contributions obtained from Gaussian line-fitting are also shown (dashed lines).

of two discrete cooperative units (*28*). The unfolding characteristics of colicin B thereby correlate with the structural and functional domain structure of this and other other membrane-active colicins (*18*, *27*). Whereas the first transition was assigned to the colicin B R/T domain, the C-domain unfolds in the second step (*28*). The unfolding of colicin B is thereby in line with that of other large proteins, whose unfolding involves discrete steps corresponding to the folding of individual domains (*1*, *33*−*35*).

*Structural Model of the Colicin B Unfolding Intermediate.* The fluorescence emission spectrum of the colicin B intermediate in 2 M GuHCl is shifted to a longer wavelength when compared to its native state (Figure 3A). Colicin B has eight tryptophan residues, five of which are present in the R/T domain. The remaining three residues are located in the channel-forming domain. Comparison with the structure of the highly homologous colicin A C-domain (cf. below) suggests that the tryptophan residues at positions 395, 439, and 449 are buried in the hydrophobic interior also in the colicin B protein (*36*, *37*). Increased fluorescence emission maxima (Figure 1A) and the loss of circular dichroism at 222 nm (Figure 3B) indicate that the unfolding intermediate at 2 M GuHCl has partially lost its native secondary and tertiary structure. Concomitantly, the DSC profile of the colicin B intermediate indicates that the well-separated peaks of the native state merge into a single broad

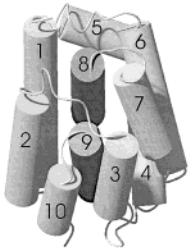


FIGURE 7: Structural model of the X-ray structure of the C-domain of colicin A (*36*). The hydrophobic helical hairpin of helices 8 and 9, which is sandwiched between two layers of helices, is shown in dark gray. The figure was prepared with MOLMOL (*59*) and POV-Ray.

transition (Figure 4). In addition, the much decreased transition temperatures indicate that the thermal stability of the intermediate is considerably reduced when compared to individual domains of native full-length colicin B (Figure 4A), a well-known effect of denaturants (*38*).

It has been shown previously that the C-terminal domain of full-length colicin B is significantly more stable in thermal unfolding experiments when compared to the R/T domain (*28*). Furthermore, at 2 M GuHCl, most of the secondary and tertiary structure of the isolated C-terminal fragment of colicin B is preserved (Figure 5A). We, therefore, suggest that the first GuHCl-induced transition ($C_{1/2} \approx 1.3$ M GuHCl) predominantly affects the R/T domain. Correspondingly, in the second step ($C_{1/2} \approx 3.1$ M), unfolding of the channel-forming domain takes place.

*Domain*−*Domain Interactions Decrease the Stability of Colicin B and Its Intermediate.* The higher stability of the isolated C-domain when compared to domains within full-length colicin B is reflected in higher midpoint of transition temperatures (Figures 4A and 6A, Table 2). In a similar manner, at pH 7.4 the thermal transition temperature of the unfolding intermediate of full-length colicin B is 20 °C reduced when compared to that of its isolated C-terminal domain (Figures 4B and 6B, Table 2). Furthermore, to completely unfold the protein, or to obtain the maximal ratio of intermediate state, higher GuHCl concentrations are required for the isolated C-terminal fragment when compared to the full-length protein (Figures 2 and 5). These observations indicate that interactions between the R/T domain and the C-terminal domain decrease the stability of full-length colicin B in both its native (*28*) and its intermediate states.

*The Global Fold of Colicin Pore-Forming Domains.* The cytotoxic functions of membrane-active colicins are attributed to the C-terminal domain, which is also the site of the pore-forming activity. Lacking a detailed structure of the folding intermediate, or of native colicin B, it is helpful to recall the high-resolution structures of other membrane-active colicins, in particular that of the C-terminal domain of colicin A. This latter sequence exhibits 71% sequence homology with the C-terminus of colicin B, and both proteins are characterized by a comparable helix content (*28*). Furthermore, high-resolution X-ray structures of full-length colicins N and Ia as well as those of the C-terminal domains of colicins A (Figure 7) and E1 all share related global folds (*36*, *39*−*41*). It is, therefore, reasonable to assume that also the C-domain of colicin B adopts very similar secondary and tertiary structures. The X-ray structures of the channel-forming domains of colicins A (Figure 7), E1, Ia, and N are

characterized by 10 helices, where 2 hydrophobic helices are surrounded by 2 layers of hydrophilic and amphipathic helices (*36*, *39*−*41*). Similar arrangements of helical layers are also found in other proteins such as citrate synthase and ribonuclease reductase (*36*).

*Identification and Characterization of the Colicin B C-Domain Intermediate.* The equilibrium unfolding studies of the isolated C-terminal domain are sigmoidal in nature and are also characterized by the presence of a small plateau region around 3.2 M GuHCl (Figure 5). The noncoincidence of the unfolding curves obtained by different techniques indicates the presence of an intermediate during the unfolding process also of this colicin fragment. During the transition from the native to the intermediate state, the three tryptophan residues of the C-terminal domain change their environment without, on average, becoming completely exposed to bulk solvent (Figure 5). In addition, the far-UV CD signal is diminished, indicating a partial loss of secondary structure (Figure 5A). Concomitantly, DSC scans of the intermediate form of the isolated C-domain show one broad transition (Figure 6B).

Structural investigations of protein folding intermediates indicate that nativelike local interactions persist, where side-chain/side-chain interactions and hydrophobic clusters, also involving residues distant in sequence, provide the nucleation sites (*4*). In a similar manner, previous unfolding studies of the colicin E1 C-terminal domain, belonging to a different group of membrane-active colicins, have shown the presence of a partially unfolded intermediate during the unfolding process using guanidine hydrochloride (*5*, *42*) or urea (*43*). Alterations in the fluorescence maxima of individual tryptophans indicate that the hydrophobic C-terminal hairpin of colicin E1 (involving helices VIII and IX) unfolds at higher denaturant concentrations when compared to the N-terminus of the C-domain (*42*).

*Subdomain Architecture of the Colicin B C-Domain.* The present studies of both GuHCl-induced and thermal unfolding show that the C-terminal domain of colicin B, which was previously thought to be made up by a single domain, in fact consists of subdomains (Figures 5A and 6A). The structure of the colicin E1 C-domain exhibits a large water-filled cavity between layers B (helices VIII, IX, and V) and C (helices III, IV, VI, and VII), which by itself is suggestive of a subdomain architecture (*39*). On the other hand, the C-domain of colicin A (Figure 7) exhibits a more tightly packed conformation where hydrophobic as well as H-bonding interactions between the three helical layers are observed (*36*). The subdomain architecture of this protein is, therefore, less obvious. It should be noted, however, that the hydrophobic helical hairpin formed by helices VIII and IX exhibits the lowest temperature factor within the colicin A C-domain, suggesting that this part of the protein is most stable.

*Functional Significance of the GuHCl Unfolding Intermediate.* The hydrophobic helical hairpins of several colicin C-domains are the most important parts of the channel-forming units. The importance of the hydrophobic helical hairpin for channel formation has been demonstrated for colicins A, E1, and Ia and the diphtheria toxin T-domain (*44*−*49*). In a related manner, protein translocase activities have been demonstrated for these proteins as long as short C-terminal domains involving the hydrophobic helical hairpin are left intact (*46*, *47*).

Channel formation by colicin A involves several steps, including electrostatic interactions with the membrane surface, partial unfolding by molten globule formation (*14*), hydrophobic insertion of the hydrophobic helical hairpin (*50*), and voltage-dependent channel opening (*51*, *52*). During membrane insertion, partial unfolding of the protein takes place, and helices I and II extend away from the other helices (*53*).

The addition of 2 M GuHCl results in a profound decrease of the thermal unfolding temperatures of full-length colicin B (Figure 4, Table 2), whereas that of the isolated C-terminal domain decreases by $\leq$8 °C even in the presence of 3.5 M denaturant (Figure 6, Table 2). Thereby the calorimetric changes of both proteins after denaturant-induced unfolding exhibit striking parallels to those observed upon acidification (*28*). The importance of acidic pH for molten globule formation, as well as membrane-association and -insertion, has been well documented for several colicins including colicin B (*23*, *54*−*57*). Therefore, the denaturant- and acid-induced unfolding intermediates appear to share important characteristics with the intermediate conformation adopted during membrane insertion (*14*).

## CONCLUSIONS

In this paper we have identified unfolding intermediates of colicin B and of its C-terminal domain. Their structural and equilibrium thermodynamic properties have been characterized. The native folds of colicin B or its C-domain are favored by an energy corresponding to about 4−7 RT when compared to their folding intermediates (Table 1). These data suggests that a small fraction of the protein spontaneously occurs as folding intermediates at pH 7.4 or at pH 4.0. In addition, these energies are small enough that the distribution between native and intermediate conformations can be significantly shifted by protein−protein or by electrostatic and hydrophobic interactions at the membrane surface (*58*).

## ACKNOWLEDGMENT

We are grateful to Luis Moroder for providing access to CD and fluorescence spectrometers and to Michael Bärmann and Prof. Erich Sackmann of the Department of Physics, Technische Universität München, Germany, for allowing us to use the DSC instrument. The contributions of Volkmar Brown, who provided the colicin B strain, and of Pieter Jasperse and Stephan Lambotte, who first established the expression and purification protocols in our laboratory, are gratefully acknowledged.

## REFERENCES

1. Privalov, P. L. (1996) *J. Mol. Biol. 258*, 707−725.
2. Fersht, A. R. (1994) *Curr. Opin. Struct. Biol. 5*, 79−84.
3. Ptitsyn, O. B. (1995) *Curr. Opin. Struct. Biol. 5*, 74−78.
4. Brockwell, D. J., Smith, D. A., and Radford, S. E. (2000) *Curr. Opin. Struct. Biol. 10*, 16−25.
5. Steer, B. A., and Merrill, A. R. (1997) *Biochemistry 36*, 3037−3046.
6. Udgaonkar, J. B., and Baldwin, R. L. (1995) *Biochemistry 34*, 4088−4096.
7. Hughson, F. M., Wright, P. E., and Baldwin, R. L. (1990) *Science 249*, 1544−1548.
8. Galtzitskaya, O. V., Ivanov, D. N., and Finkelstein, A. V. (2001) *FEBS Lett. 489*, 113−118.

9. Grimsley, J. K., Scholtz, J. M., Pace, C. N., and Wild, J. R. (1997) *Biochemistry 36*, 14366−14374.
10. Popot, J. L., and Engelman, D. M. (2000) *Annu. Rev. Biochem. 69*, 881−922.
11. Bogdanov, M., and Dowhan, W. (1999) *J. Biol. Chem. 274*, 36827−36830.
12. Kuwajima, K. (1996) *FASEB J. 10*, 109.
13. Dill, K. A., and Stigter, D. (1995) *Adv. Protein Chem. 46*, 59−104.
14. van der Goot, F. G., Gonzalez-Manas, J. M., Lakey, J. H., and Pattus, F. (1991) *Nature 354*, 408−410.
15. von Heijne, G. (1995) *Bioessays 17*, 25−30.
16. Minn, A. J., Vélez, P., Schendel, S. L., Liang, H., Muchmore, S. W., Fesik, S. W., Fill, M., and Thompson, C. B. (1997) *Nature 385*, 353−357.
17. Pattus, F., Massotte, D., Wilmsen, H. U., Lakey, J., Tsernoglou, D., Tucker, A., and Parker, M. W. (1990) *Experientia 46*, 180−192.
18. Lakey, J. H., van der Goot, F. G., and Pattus, F. (1994) *Toxicology 87*, 85−108.
19. Schramm, E., Mende, H., Braun, V., and Kamp, R. M. (1987) *J. Bacteriol. 169*, 3350−3357.
20. Lazdunski, C. J. (1995) *Mol. Microbiol. 16*, 1059−1066.
21. Gouaux, E. (1997) *Structure 5*, 313−317.
22. Pressler, U., Braun, V., Wittmann-Liebold, B., and Benz, R. (1986) *J. Biol. Chem. 261*, 2654−2659.
23. Bullock, J. O., Armstrong, S. K., Shear, J. L., Lies, D. P., and McIntosh, M. A. (1990) *J. Memb. Biol. 114*, 79−95.
24. Lambotte, S., Jasperse, P., and Bechinger, B. (1998) *Biochemistry 37*, 16−22.
25. Lakey, J. H., van der Goot, F. G., and Pattus, F. (1994) *Toxicology 87*, 85−108.
26. Stroud, R. M., Reiling, K., Wiener, M., and Freymann, D. (1998) *Curr. Opin. Struct. Biol. 8*, 525−533.
27. Kienker, P. K., Qiu, X., Slatin, S. L., Finkelstein, A., and Jakes, K. S. (1997) *J. Membr. Biol. 157*, 27−37.
28. Ortega, A., Lambotte, S., and Bechinger, B. (2001) *J. Biol. Chem. 276*, 13563−13572.
29. Muga, A., Gonzalez-Manas, J. M., Lakey, J. H., Pattus, F., and Surewicz, W. K. (1993) *J. Biol. Chem. 268*, 1553−1557.
30. Pace, C. N., Shirely, B. A., and Thomson, J. A. (1989) in *Protein structure—A practical approach* (Creighton, T. E., Ed.) pp 311−329, IRL Press, Oxford.
31. Beasty, A. M., Hurle, M. R., Manz, J. T., Stackhouse, T., Onuffer, J. J., and Matthews, C. R. (1986) *Biochemistry 25*, 2965−2974.
32. White, S. H., and Wimley, W. C. (1999) *Annu. Rev. Biophys. Biomol. Struct. 28*, 319−365.
33. Garel, J. R. (1995) in *Protein Folding* (Creighton, T. E., Ed.) pp 405−454, W. H. Freeman and Co., New York.
34. Abkevich, V. I., Gutin, A. M., and Schaknovich, E. I. (1995) *Protein Sci. 4*, 1167−1177.
35. Dobson, C. M. (1995) *Struct. Biol. 2*, 513−517.
36. Parker, M. W., Postma, J. P., Pattus, F., Tucker, A. D., and Tsernoglou, D. (1992) *J. Mol. Biol. 224*, 639−657.
37. Lakey, J. H., Massotte, D., Heitz, F., Dasseux, J. L., Faucon, J. F., Parker, M. W., and Pattus, H. (1991) *Eur. J. Biochem. 196*, 599−607.
38. Ramsay, G., and Freire, E. (1990) *Biochemistry 29*, 8677−8683.
39. Elkins, P., Bunker, A., Cramer, W. A., and Stauffacher, C. V. (1997) *Structure 5*, 443−458.
40. Weiner, M., Freymann, D., Ghosh, P., and Stroud, R. M. (1997) *Nature 385*, 461−464.
41. Vetter, I. R., Parker, M. W., Tucker, A. D., Lakey, J. H., Pattus, F., and Tsernoglou, D. (1998) *Structure 6*, 863−874.
42. Steer, B. A., and Merrill, A. R. (1995) *Biochemistry 34*, 7225−7233.
43. Steer, B. A., DiNardo, A. A., and Errill, A. R. (1999) *Biochem. J. 340*, 631−638.
44. Nardi, A., Slatin, S. L., Baty, D., and Duche, D. (2001) *J. Mol. Biol. 307*, 1293−1303.
45. Slatin, S. L., Qui, X. Q., Jakes, K. S., and Finkelstein, A. (1994) *Nature 371*, 158−161.
46. Huynh, P. D., Ciu, C., Zhan, H., Oh, K. J., Collier, R. J., and Finkelstein, A. (1997) *J. Gen. Physiol. 110*, 229−242.
47. Jakes, K. S., Kienker, P. K., and Finkelstein, A. (1999) *Q. Rev. Biophys. 32*, 189−205.
48. Baty, D., Knibiehler, M., Verheij, H., Pattus, F., Shire, D., Bernadac, A., and Lazdunski, C. (1987) *Proc. Natl. Acad. Sci. U.S.A. 84*, 1152−1156.
49. Liu, Q. R., Crozel, V., Levinthal, F., Slatin, S., Finkelstein, A., and Levinthal, C. (1986) *Proteins: Struct., Funct., Genet. 1*, 218−229.
50. Parker, M. W., Pattus, F., Tucker, A. D., and Tsernoglou, D. (1989) *Nature 337*, 93−96.
51. Letellier, L. (1992) *Biochim. Biophys. Acta 1101*, 218−220.
52. Collarini, M., Amblard, G., Lazdunski, C., and Pattus, F. (1987) *Eur. Biophys. J. 14*, 147−153.
53. Lakey, J. H., Duche, D., Gonzalez-Manas, J. M., Baty, D., and Pattus, F. (1993) *J. Mol. Biol. 230*, 1055−1067.
54. Pattus, F., Martinez, M. C., Dargent, B., Cavard, D., Verger, R., and Lazdunski, C. (1983) *Biochemistry 22*, 5698−5703.
55. Frenette, M., Knibiehler, M., Baty, D., Geli, V., Pattus, F., Verger, R., and Lazdunski, C. (1989) *Biochemistry 28*, 2509−2514.
56. Bullock, J. O. (1992) *J. Membr. Biol. 125*, 255−271.
57. Mel, S. F., and Stroud, R. M. (1993) *Biochemistry 32*, 2082−2089.
58. Lakey, J. H., Parker, M. W., Gonzalez-Manas, J. M., Duche, D., Vriend, G., Baty, D., and Pattus, F. (1994) *Eur. J. Biochem. 220*, 155−163.
59. Koradi, R., Billeter, M., and Wüthrich, K. (1996) *J. Mol. Graphics 14*, 51−55.


BI0115784